

# Model-Based Estimation of Ultrasonic Echoes

## Part I: Analysis and Algorithms

Ramazan Demirli, *Student Member, IEEE*, and Jafar Saniie, *Senior Member, IEEE*

**Abstract**—The patterns of ultrasonic backscattered echoes represent valuable information pertaining to the geometric shape, size, and orientation of the reflectors as well as the microstructure of the propagation path. Accurate estimation of the ultrasonic echo pattern is essential in determining the object/propagation path properties. In this study, we model ultrasonic backscattered echoes in terms of superimposed Gaussian echoes corrupted by noise. Each Gaussian echo in the model is a nonlinear function of a set of parameters: echo bandwidth, arrival time, center frequency, amplitude, and phase. These parameters are sensitive to the echo shape and can be linked to the physical properties of reflectors and frequency characteristics of the propagation path. We address the estimation of these parameters using the maximum likelihood estimation (MLE) principle, assuming that all of the parameters describing the shape of the echo are unknown but deterministic. In cases for which noise is characterized as white Gaussian, the MLE problem simplifies to a least squares (LS) estimation problem. The iterative LS optimization algorithms when applied to superimposed echoes suffer from the problem of convergence and exponential growth in computation as the number of echoes increases. In this investigation, we have developed expectation maximization (EM)-based algorithms to estimate ultrasonic signals in terms of Gaussian echoes. The EM algorithms translate the complicated superimposed echoes estimation into isolated echo estimations, providing computational versatility. The algorithm outperforms the LS methods in terms of independence to the initial guess and convergence to the optimal solution, and it resolves closely spaced overlapping echoes.

### I. INTRODUCTION

BY INSPECTING the backscattered echoes, the ultrasonic pulse-echo method aims to characterize the propagation path and/or to determine the physical properties of reflectors in terms of their location, size, orientation, and microstructure. The extraction of the information related to various properties of reflectors requires models that explain the formation of echoes. The formation of backscattered echoes can be studied through the pulse-echo system for which the transducer impulse response (pulse-echo wavelet) is the input, and the received backscattered echoes are the output. This linear system can be further decomposed into the propagation path response (propagation filter) and the target response. The propagation filter represents the frequency effects of the propagation path caused by the frequency-dependent ab-

sorption and scattering [1]. These effects can be observed in terms of frequency dispersion, diffraction, phase shift, and attenuation of the original pulse-echo wavelet. The target response can be attributed to the following factors: target location with reference to transducer beam field; target acoustical impedance; and geometric shape, size, and orientation [2]. The target response is observed in terms of reflection, attenuation, and phase inversion of the original pulse-echo wavelet.

The signal parameters of ultrasonic echoes are sensitive to the target and propagation path response as well as to the transducer pulse-echo wavelet. The backscattered echo from an isolated reflector can be considered as the time-shifted, frequency-dissipated, and energy-attenuated replica of the transducer pulse-echo wavelet. The time of arrival (TOA) of the echo can be linked to the location of the target when the path is homogeneous. The center frequency of the echo with reference to the center frequency of the pulse-echo wavelet can be attributed to the propagation filter response. These two parameters of ultrasonic echoes, TOA, and center frequency are of special interest and have been widely used in ultrasonic applications [3], [4].

Many ultrasonic testing applications are based on the estimation of the TOA, time of flight (TOF), or the time-difference of arrival (TDOA) of ultrasonic echoes. Target localization relies on the estimation of the TOA of an echo reflected from a target (flaw, layer ... etc.) identified by its impedance mismatch on the propagation path. Because the transducer impulse response obscures the exact location of the target, further processing, e.g., deconvolution, of the target echo is needed to estimate high resolution TOA [5]. The thickness measurement requires estimating the TDOA of echoes reflected from the boundaries of a layer whose ultrasonic velocity is known. Similarly, the velocity measurement requires estimating the TDOA of echoes reflected from the boundaries of a layer whose thickness is known [3]. Surface profiling is another TOF estimation-based application in which the surface of an object is exposed to narrowband ultrasonic pulses generated by a low frequency airborne transducer. The received echoes are inspected to determine their TOF at the grids of the object surface. Then, the TOFs are mapped to the intensity levels to form the profile image [6], [7]. Subsample time delay estimation addresses the estimation of time delays between different ensembles of the measured ultrasonic signal. In NDE (nondestructive evaluation) testing, many samples of ultrasonic signals are collected and averaged to improve the SNR. Subsample time delays arise

Manuscript received June 28, 2000; accepted December 21, 2000.

The authors are with the Department of Electrical and Computer Engineering, Illinois Institute of Technology, Chicago, IL 60616-3793 (e-mail: sansonic@ece.iit.edu).

between the ensembles because of the imperfections of the measurement system or the unstable conditions in the propagation path. The time delays of all of the samples need to be estimated so that the signals can be aligned on the time axis for better averaging as well as for better TOF estimation [7], [9].

The methods used to estimate TOA, TOF, TDOA, and subsample time delays in ultrasonic applications are mainly based on the cross-correlation method. The cross-correlation method stems from the “matched filtering” approach, where a linear time invariant filter is designed to produce maxima at the TOA of the received echo. The received echo is assumed to be a time-shifted, amplitude-scaled, and noise-corrupted version of the reference echo. The cross-correlation integral is computed by shifting the reference echo and integrating over the received signal. It would presumably produce a peak at the TOA of the received signal because the correlation of the received signal with the reference signal at that time instant is expected to be the maximum. It should be noted that the cross-correlation method is optimal when 1) the noise in the received signal is characterized by white Gaussian noise (WGN) and 2) the received signal is the time-shifted, amplitude-scaled replica of the reference signal. Therefore, any situation that violates either of those two assumptions limits the use of the cross-correlation method.

The major shortcoming of the cross-correlation method in TOF estimation is the unavailability of the reference signal. Theoretically, the transducer impulse response is the reference signal, but the exact shape of the impulse response is not known. To overcome this, some specific shape, depending on transducer frequency characteristics, is assumed for the reference echo. In general, a measurement for the reference echo is performed prior to the actual experiment [1]. On the other hand, even if the reference signal is available, the received echo might have undergone a shape distortion. The shape distortion may appear in the form of frequency dissipation or phase shift or envelope distortion with respect to the reference echo. The received echoes disperse in time as the ultrasound travels deep into the material, introducing a frequency downshift [10]. Therefore, the cross-correlation method in these cases may become inefficient.

Another major limitation of the cross-correlation method in TOF estimation is resolution, which is essential in some applications. In the case of subsample time delay estimation and surface profiling, the resolution of the estimator needs to be high (fine) to track small changes in TOA. However, the resolution of the cross-correlation estimator is the sampling interval. This restricts the direct use of cross-correlation method in subsample time delay estimation. Further processing of cross correlation, such as interpolation, parabolic approximation near the peak, is usually employed to obtain high resolution estimates [7], [9].

Another important parameter of an ultrasonic echo is the center frequency. The center frequency of an ultrasonic echo is influenced by the transducer center frequency as

well as the frequency characteristics of the propagation path. The frequency modification of the path is due to the frequency-dependent absorption and scattering, which is, in turn, governed by the microstructure of the material [11]. Many parameters of acoustic propagation that are related to the characterization require an accurate estimation of frequency [12]. In particular, the acoustic attenuation coefficient, mean scatterer spacing, backscattering coefficient, and materials quality factor are all used for tissue characterization in medical ultrasound or material characterization in NDE.

The ultrasonic attenuation coefficient, for example, characterizes the frequency-dependent absorption and scattering. The attenuation has been shown to be almost linearly dependent on frequency for soft tissues [13]. In solids, e.g., polycrystalline metals consisting of cubic or hexagonal, tightly packed grains, the attenuation coefficient depends on the third power of the frequency when the testing is in the Rayleigh scattering region [2], [11]. These effects appear in the form of a frequency downshift in the spectrum of the backscattered echoes as they propagate deep into the material or tissue. This parameter can be deduced from the center frequency or the maximum frequency of the power spectral density (PSD) or from the inspection of PSD as a whole [10]. However, the accuracy and resolution of the center frequency rely on the accuracy and resolution of the PSD estimation. The bias and high variance in PSD introduced by the estimation method will degrade the accuracy of the center frequency estimation. Model-based time domain methods may be an alternative to PSD methods in estimating the frequency of ultrasonic echoes. Although ultrasonic backscattered echoes are not stationary in general, they are close to locally stationary over small ranges [14]. Then, over these small ranges, the frequency of the echo can be represented by the sum of sinusoidal signals. This time domain approach to frequency estimation will be presented in the model-based estimation context.

In this study, we use a parametric signal model to analyze ultrasonic backscattered echoes. This model is sensitive to the signal characteristics, i.e., TOA, center frequency, phase, amplitude, and bandwidth of the ultrasonic echo. Several advantages have been projected using the signal model. First, high-resolution parameter estimates can be achieved. Second, the accuracy of the estimation can be evaluated. Third, the analytical relationship between model parameters and physical parameters of the system can be established.

The remainder of this paper is organized as follows. The signal model is presented in Section II. Section III addresses the MLE of an ultrasonic echo in terms of model parameters. Section IV analyzes the performance of the estimation through analytical methods. In Section V, the estimation problem is generalized to the estimation of a known number of superimposed model echoes using EM algorithms. The performance of the algorithms is tested and compared with that of the LS methods for simulated and experimental ultrasonic echoes.

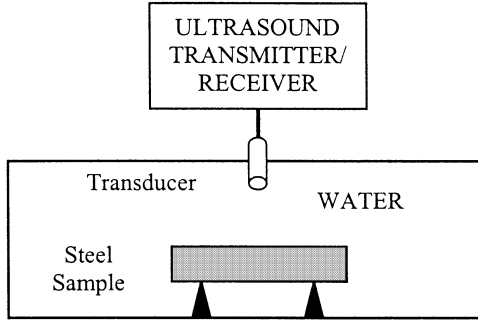


Fig. 1. Experimental setup for a planar surface reflector.

## II. GAUSSIAN ECHO MODEL

In pulse-echo ultrasonic testing, the backscattered echo from a flat surface reflector can be modeled as

$$s(\theta; t) = \beta e^{-\alpha(t-\tau)^2} \cos(2\pi f_c(t-\tau) + \phi) \quad (1)$$

$$\theta = [\alpha \ \tau \ f_c \ \phi \ \beta].$$

Because of its Gaussian-shaped envelope, this model will be referred to as a Gaussian echo model. The signal parameters of the echo are  $\alpha$  = bandwidth factor,  $\tau$  = arrival time,  $f_c$  = center frequency,  $\phi$  = phase, and  $\beta$  = amplitude. These parameters have intuitive meanings for an ideal surface reflector in a homogeneous propagation path. Time of arrival  $\tau$  is related to the location of the reflector. The bandwidth factor  $\alpha$  determines the bandwidth of the echo or the time duration of the echo in the time domain. The center frequency  $f_c$  is governed by the transducer center frequency and the frequency characteristics of the propagation path. The echo has a specific amplitude  $\beta$  and phase  $\phi$  accounting for the impedance, size, and orientation of the reflector.

To demonstrate the feasibility of the model, an experimental setup, shown in Fig. 1, has been used. A block of steel is positioned in the far field of a broadband 5-MHz transducer (0.5-in. diameter, unfocused, manufactured by Panametric) in the water tank. The measured echo (using the 5052PR Panametric ultrasonic pulser and data) is sampled at 100 MHz with an 8-bit resolution. The reflection from the front surface is shown in Fig. 2(a), and its magnitude spectrum is shown in Fig. 2(b). Fig. 2(c) depicts the estimated echo by fitting a Gaussian echo model to the experimental echo. The estimated parameters of this echo are bandwidth factor  $\alpha = 25$  (MHz)<sup>2</sup>, arrival time  $\tau = 1.07 \mu s$ , center frequency  $f_c = 5.34$  MHz, phase  $\phi = 0.87$  rad, and amplitude  $\beta = 1.01$ . The estimation SNR, i.e., the energy of the estimated signal over the energy of the estimation error, is 21.25 dB. The magnitude spectrum of the estimated echo is shown in Fig. 2(d), which is in good agreement with the magnitude spectrum of the measured echo.

To account for noise effects in estimation, a noise process can be included in the model. The noise comes from measurement and can be characterized as the additive WGN [2]. Then, the ultrasonic echo from a flat surface

reflector can be modeled as

$$x(t) = s(\theta; t) + \nu(t) \quad (2)$$

where  $s(\cdot)$  denotes the Gaussian echo model (1) and  $\nu(t)$  denotes the additive WGN process. This model can be extended to a multiple echo model to represent echoes from a known number of reflectors. Assuming a Gaussian echo for each reflector, the received echoes can be modeled by M-superimposed Gaussian echoes:

$$y(t) = \sum_{m=1}^M s(\theta_m; t) + \nu(t). \quad (3)$$

Note that each parameter vector  $\theta_m$  completely defines the shape and location of the corresponding echo. This system is illustrated schematically in Fig. 3.

In this study, we address the estimation of parameters of Gaussian echoes when the measured backscattered signal contains additive WGN. To proceed further with the estimation issues, we need to define and develop explicit solution for some useful signal properties such as the echo energy, SNR, and the echo bandwidth.

### A. Energy, SNR, and Bandwidth of the Gaussian Echo

The magnitude spectrum of the normalized ( $\beta = 1$ ) and zero-phase ( $\phi = 0$ ) Gaussian echo wavelet (1) can be written as

$$|S(f)| = \frac{1}{2} \sqrt{\frac{\pi}{\alpha}} \left( e^{\frac{-\pi^2(f-f_c)^2}{\alpha}} + e^{\frac{-\pi^2(f+f_c)^2}{\alpha}} \right) \quad (4)$$

where  $f$  denotes the frequency variable. The energy spectrum is obtained by taking the square of (4) as

$$P_{ss}(f) = \frac{\pi}{4\alpha} \left( e^{\frac{-2\pi^2(f-f_c)^2}{\alpha}} + e^{\frac{-2\pi^2(f+f_c)^2}{\alpha}} + 2e^{\frac{-2\pi^2f_c^2}{\alpha}} e^{\frac{-2\pi^2f^2}{\alpha}} \right). \quad (5)$$

Finally, the echo energy can be obtained by integrating the energy spectrum in the frequency range  $[-\infty, \infty]$ :

$$E_s = \frac{1}{2} \sqrt{\frac{\pi}{2\alpha}} \left( 1 + e^{\frac{-2\pi^2f_c^2}{\alpha}} \right). \quad (6)$$

The exponential term in (6) is negligible for bandpass signals in which the center frequency is greater than the bandwidth. For the exponential term to have less than 1% of the energy, the condition  $f_c^2 \geq 0.24\alpha$  must be satisfied. Based on this assumption and taking echo amplitude  $\beta$  into account, the energy formula for the echo can be further simplified as

$$E_s = \frac{\beta^2}{2} \sqrt{\frac{\pi}{2\alpha}}. \quad (7)$$

Note that the echo energy depends only on the amplitude and bandwidth factor. For an ultrasonic signal represented

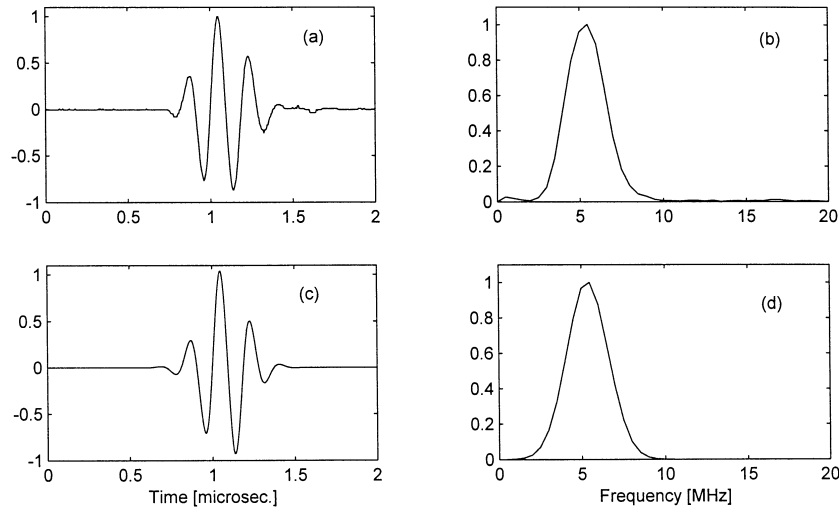


Fig. 2. a) The measured echo reflected from the front surface of a steel sample. b) The normalized magnitude spectrum of the echo in (a). c) The estimated echo in (a) by fitting a Gaussian echo model. d) The normalized magnitude spectrum of the echo in (c).

by M-Gaussian echoes, the energy can be calculated as the sum of the energies of the composing echo plus the cross energy terms, i.e.,  $E_{ij} = \int s(\theta_i; t)s(\theta_j; t)dt$  for  $i \neq j$ . Meanwhile, the SNR can be determined explicitly in the case of WGN with variance  $\sigma_\nu^2$  as

$$SNR = 10 \log \left( \frac{E_s}{\sigma_\nu^2} \right) [dB]. \quad (8)$$

The bandwidth of the echo can be deduced from the energy spectrum (5). The great majority of the energy is confined around the center frequency such that the signal energy far away from center frequency is negligible. For a Gaussian echo, the 98% bandwidth that contains 98% of the signal energy is

$$BW_{98\%} = 0.382\sqrt{\alpha}. \quad (9)$$

In summary, when the ultrasonic echo is decomposed by Gaussian echoes, one can assess the energy, SNR, and bandwidth of the echo in terms of Gaussian echo parameters. However, the determination of echo parameters from the measured signal requires estimation. The estimation problem is presented in the next section.

### III. MAXIMUM LIKELIHOOD ESTIMATION OF AN ULTRASONIC ECHO

For computational purposes, the observation model (2) for an ultrasonic echo can be written in a discrete form as

$$x = s(\theta) + \nu \quad (10)$$

where  $x \in \Re^N$  is a vector of observations,  $\nu \in \Re^N$  is a WGN sequence, and  $s(\theta): \theta \in \Re^5 \rightarrow s(\theta) \in \Re^N$  is a Gaussian echo vector defined by the model

$$s(\theta; t(nT)) = \beta e^{-\alpha(t(nT)-\tau)^2} \cos\{2\pi f_c(t(nT) - \tau) + \phi\}, \\ \text{for } n = 0, 1, 2, \dots, N-1 \quad (11)$$

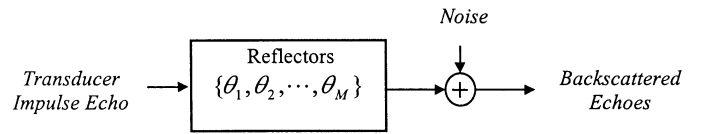


Fig. 3. Parametric signal model for ultrasonic backscattered echoes.

where  $t(nT)$  are the discrete samples of the time variable  $t$  and  $T$  is the sampling interval. The parameters of the echo are stored in the parameter vector,  $\theta = [\alpha \ \tau \ f_c \ \phi \ \beta]$ .

Our goal is to estimate the parameter vector  $\theta$  given the observations in  $x$ . Several issues arise with the parameter estimation problem. First, the transformation from parameter space to signal space, although appropriately defined by the Gaussian echo model, is nonlinear. Hence, the reverse process, the transformation from signal space to parameter space is also nonlinear and has no explicit solution. Second, the noise embedded on the measured signal obscures the estimation of parameters. This degradation needs to be quantified to assess the accuracy of estimation. In this paper, we address the nonlinear parameter estimation problem in the MLE framework. Then, we evaluate the performance of estimation using analytical methods. Assuming all of the observations ( $x$ ) are independent and identically distributed (iid), their joint probability density function (pdf) obeys the normal distribution

$$p(x : \theta) = \frac{1}{(2\pi)^{\frac{N}{2}} |C(\theta)|^{\frac{1}{2}}} \\ \cdot \exp \left\{ -\frac{1}{2}(x - \mu(\theta))^T C^{-1}(\theta)(x - \mu(\theta)) \right\} \quad (12)$$

where  $\mu(\theta) = E\{s(\theta) + \nu\}$  is the mean vector and  $C(\theta) = E\{(x - \mu(\theta))(x - \mu(\theta))^T\}$  is the covariance matrix of observations. This joint pdf with respect to the parameter vector  $\theta$  is known as the likelihood function. The MLE of  $\theta$  is defined as the value of the parameter vector that max-

imizes the likelihood function. For the case of WGN and the constant parameter vector of the observation model in (10), maximizing the likelihood function simplifies to minimizing the LS function:

$$J(\theta) = (x - s(\theta))^T(x - s(\theta)) = \|x - s(\theta)\|^2. \quad (13)$$

The MLE of  $\theta$  can be found by minimizing this objective function, which only uses the observed data  $x$  and the model  $s(\theta)$ . However, the objective function is nonlinear in the parameter vector  $\theta$ , offering no immediate solution. This optimization problem is recognized as an unconstrained nonlinear LS problem because there is no constrained region provided on the parameter vector. Iterative optimization algorithms are available in scientific program libraries for nonlinear LS problems. These algorithms start with an initial guess for the parameter vector then improve it in such a fashion as to minimize the objective function. The minimum value of the objective function (global minimum) provides the optimal solution. However, there may be local minima as well. Depending on the initial starting point, the algorithm may remain in one of the local minima, yielding a suboptimal solution. Special care may be needed to ensure optimal convergence specific to the problem at hand.

We have explored the minimization of the objective function (13) using two different optimization methods: simplex search and Levenberg-Marquardt. The simplex search method [15] (a first-order method) uses only function evaluations in iterating the parameter vector. This method is known for its immunity to local minima but requires significant iterations when compared with second-order methods. The Levenberg-Marquardt method [16] (a second-order method), in addition to function evaluations, uses gradient information as well as the Hessian matrix approximation to move on to the next iteration. This method, although faster than the simplex search, is sensitive to local minima. It requires a good initial guess to converge to the optimal solution [17].

In this study, we have developed a Gauss Newton (GN) algorithm tailored to our specific problem for fast computation. Taking advantage of the echo model, the GN iteration formula [18] for estimation of the parameter vector can be written as

$$\theta^{(k+1)} = \theta^{(k)} + (H^T(\theta^{(k)})H(\theta^{(k)}))^{-1}H^T(\theta^{(k)})(x - s(\theta^{(k)})) \quad (14)$$

where  $H(\theta)$  represents the gradients of the model with respect to parameters in the parameter vector  $\theta = [\alpha \ \tau \ f_c \ \phi \ \beta]$ . In implementing the iteration formula, the gradients can be calculated analytically to speed up computations. The analytical gradients of a Gaussian echo are derived in the Appendix A [see (A2)–(A6)]. Furthermore, the inversion of the term  $H^T(\theta)H(\theta)$  in the iteration formula can be bypassed by using its analytical equivalent [see (A8), Appendix A]. Finally, the iteration is terminated when the norm of the improvement in the parameter vector

is less than a preset tolerance. In summary, the GN algorithm for parameter estimation of a Gaussian echo can be implemented in the following computational steps.

- Step 1. Make an initial guess for the parameter vector  $\theta^{(0)}$  and set  $k = 0$  (iteration number).
- Step 2. Compute the gradients  $H(\theta^{(k)})$  and the model  $s(\theta^{(k)})$ .
- Step 3. Iterate the parameter vector:  

$$\theta^{(k+1)} = \theta^{(k)} + (H^T(\theta^{(k)})H(\theta^{(k)}))^{-1}H^T(\theta^{(k)})(x - s(\theta^{(k)})).$$
- Step 4. Check convergence criterion.  
If  $\|\theta^{(k+1)} - \theta^{(k)}\| < \text{tolerance}$ , then stop.
- Step 5. Set  $k \rightarrow k + 1$  and go to Step 2.

#### A. Parameter Estimation Results and Discussions

The performance of the GN algorithm is tested and compared with the simplex search algorithm for simulated Gaussian echoes in WGN. An ultrasonic echo (11) with bandwidth factor  $\alpha = 25$  (MHz)<sup>2</sup> (the 98% bandwidth is 1.91 MHz), arrival time  $\tau = 1 \mu\text{s}$ , center frequency  $f_c = 5$  MHz, phase  $\phi = 1$  rad, and amplitude  $\beta = 1$  is simulated when  $\theta = [25 \ 1 \ 5 \ 1 \ 1]$ . This echo is sampled at the sampling frequency  $f_s = 200$  MHz and stored in a signal vector  $s$ . A realization of a zero mean WGN sequence with variance  $\sigma^2$  is added to the echo to form an observation vector  $x$ . Different variances of noise sequences are generated to simulate echoes with SNR of 20, 10, and 5 dB. The SNR of the echo is computed using (8). Then, the GN and simplex search algorithms are applied to estimate the echo parameters. The initial guess,  $\theta^{(0)} = [15 \ 0.7 \ 3 \ 0 \ 0.7]$ , is provided for the parameter vector in the algorithms. The simulated and estimated echoes for different SNRs are plotted in Fig. 4. For comparison, the original echo used in simulation (solid line) is also plotted in the figure along with the estimated echoes (dotted line). The estimation results for both methods are tabulated in Table I in terms of estimated parameters, the mean square error, and the number of iterations.

The estimation of a noise-free echo [Fig. 4(a)] is achieved with 100% accuracy [Fig. 4(b)]. However, the estimation of a noisy echo with a SNR of 20 dB [Fig. 4(c)] is not the same as the original because the noise distorts the shape of the echo, obscuring actual echo parameters. As the SNR worsens, the accuracy of the parameter estimation degrades as expected [for example, see Fig. 4(h)]. However, for each echo with different SNR, the two fundamentally different algorithms yield the same parameter vector, supporting the idea of optimality for estimated parameters. In fact, any initial guess relatively close to the actual parameter vector would easily yield the optimum. The initial guess far from the optimum may result in a suboptimal solution because of the local minima. This is demonstrated using a very poor initial guess,  $\theta^{(0)} = [2 \ 0.3 \ 3 \ 0 \ 0.7]$ . The GN algorithm produced an estimate of  $\theta^* = [7 \ 0.6 \ 4 \ 0.3 \ 0.6]$ , far from the optimal. However, the simplex search method, using the same initial guess, achieves the optimum even though it takes

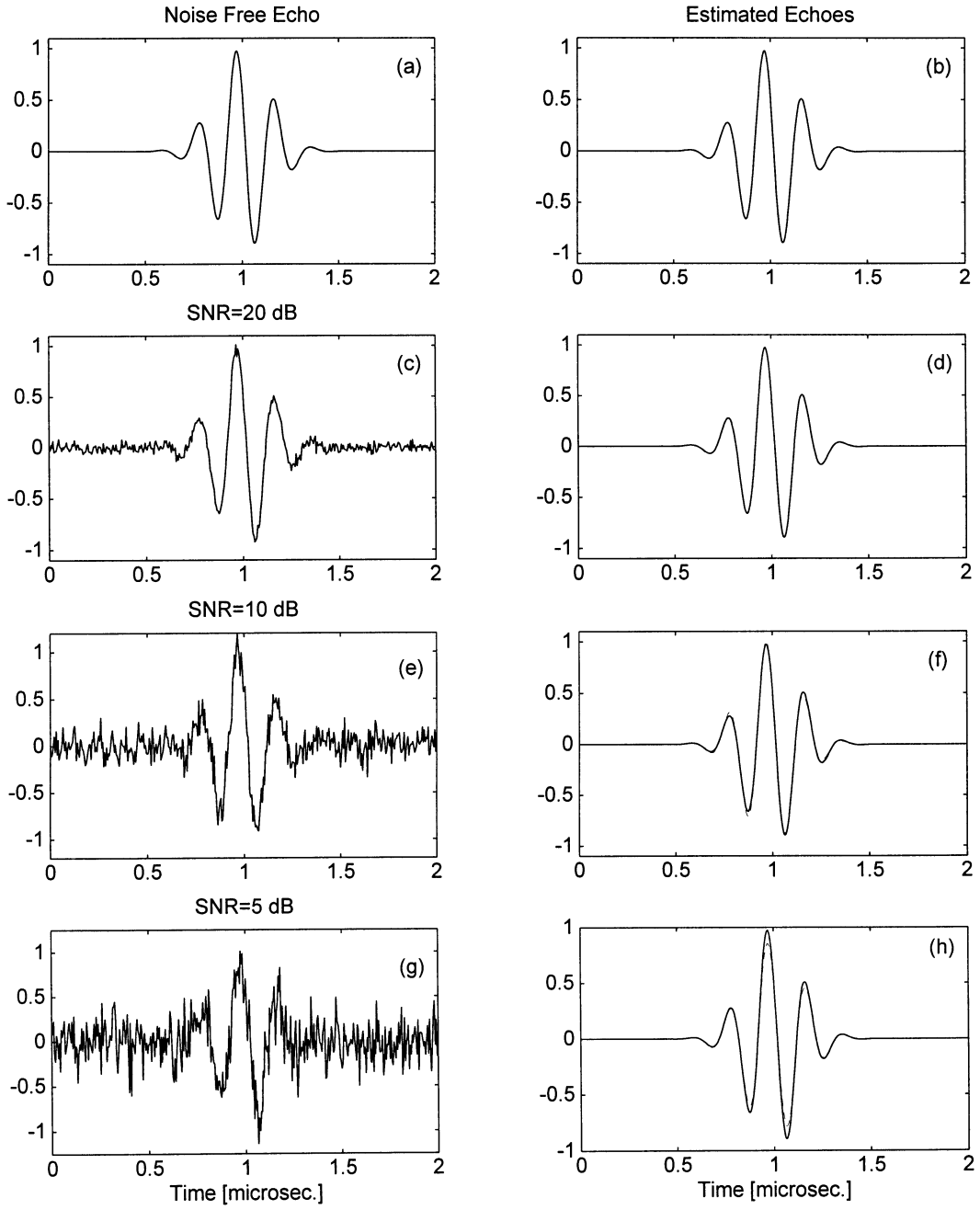


Fig. 4. a) Noise-free echo. b) The estimated echo of the signal (a) plotted in a dotted line and the original echo plotted in a solid line. c) The echo with a SNR of 20 dB. d) The estimated echo of the signal (c) plotted in a dotted line and the original echo plotted in a solid line. e) The echo with a SNR of 10 dB. f) The estimated echo of the signal (d) plotted in a dotted line and the original echo plotted in a solid line. g) The echo with a SNR of 5 dB. h) The estimated echo of the signal (g) plotted in a dotted line and the original echo plotted in a solid line.

significant iterations. A good initial guess not only guarantees the optimal solution but also saves extra computation. A systematic procedure can be developed to make a good initial guess for the echo parameters. This is not a difficult task because the parameters of the echo are closely related to the transducer impulse response. The maximum amplitude of the observation can be taken as an initial guess for the amplitude of the echo. The arrival time of a Gaussian echo is usually around the neighborhood of the maximum value. The initial guess for center frequency and

bandwidth can be made based on zero-crossings and time duration of the echo. Using this procedure, an initial guess,  $\theta^{(0)} = [15 \ 0.9 \ 4.6 \ 0 \ 0.9]$ , is made for the echo with a SNR of 5 dB [Fig. 4(g)] and provided to the GN algorithm. The algorithm achieves the optimal solution with fewer numbers of iterations.

In conclusion, the parameter estimation of a Gaussian echo when using a fair initial guess is robust and computationally efficient. Although the simulation results support the optimality of the estimated parameters, analyti-

TABLE I  
PARAMETER ESTIMATION RESULTS USING THE GN AND SIMPLEX SEARCH METHODS.

	Bandwidth factor [(MHz) <sup>2</sup> ]	Arrival time (μs)	Center frequency (MHz)	Phase (rad)	Amplitude	Mean square error	Number of iterations
Actual parameters	25.0000	1.0000	5.0000	1.0000	1.0000		
Initial guess	15.0000	0.7000	3.0000	0.0000	0.8000		
Noise free							
GN	25.0000	1.0000	5.0000	1.0000	1.0000	2.00E-13	16
Simplex search	25.0000	1.0000	5.0000	1.0000	1.0000	2.00E-13	624
20-dB SNR							
GN	25.0898	0.9998	4.9936	7.2810	0.9919	4.54E-01	18
Simplex search	25.0898	0.9998	4.9936	7.2810	0.9919	4.54E-01	654
10-dB SNR							
GN	25.5119	0.9909	5.0271	6.9725	1.0193	4.95E+00	16
Simplex search	25.5119	0.9909	5.0271	6.9725	1.0193	4.95E+00	752
5-dB SNR							
GN	23.1312	0.9998	4.9869	0.9315	0.8736	1.61E+01	22
Simplex search	23.1312	0.9998	4.9869	0.9315	0.8736	1.61E+01	606

cal methods can be applied for formal proof. This issue is addressed in the next section.

#### IV. CRLB BOUNDS FOR PERFORMANCE ANALYSIS

We have observed that the estimated parameters by both of the methods (GN and simplex search) show a high degree of consistency with the actual echo parameters used in simulations. In general, any optimum parameter estimator should be unbiased, i.e., on the average, it should yield the true value of the parameter. Furthermore, the variance of the optimum estimator should be less than that of all of the other estimators. The Cramer-Rao Lower Bounds (CRLB) provide a benchmark on the variances of the estimators. That is, in the presence of noise, the variances of estimators cannot be smaller than those prescribed by the CRLB. The CRLB for a vector parameter  $\theta$  is defined by the following inequality [18]:

$$\text{var}(\hat{\theta}_i) \geq [I^{-1}(\theta)]_{ii} \quad (15)$$

where  $I(\theta)$  is the Fisher information matrix defined as

$$[I(\theta)]_{ij} = -E\left[\frac{\partial^2 \ln p(x; \theta)}{\partial \theta_i \partial \theta_j}\right] \quad (16)$$

where  $\ln p(x; \theta)$  is the log-likelihood function (12). For any Gaussian observation model, where  $x$  is normally distributed as  $N(s(\theta), \sigma^2 I)$ , the Fisher information matrix can be written as [18]

$$I(\theta) = \frac{1}{\sigma^2} H^T(\theta) H(\theta) \quad (17)$$

where  $H(\theta)$  represents the gradients of the Gaussian echo model [for details, see (A7) in Appendix A]. The analytical derivation of the Fisher information matrix is also given in the Appendix A, (A9). The terms along the diagonal of the inverse Fisher information matrix [(A10) in Appendix

A] yields the CRLB analytical bounds on the variances of estimated parameters:

$$\text{var}(\hat{\alpha}) \geq \frac{8\alpha^2}{f_s \varsigma} \quad (18a)$$

$$\text{var}(\hat{\tau}) \geq \frac{1}{f_s \varsigma \alpha} \quad (18b)$$

$$\text{var}(\hat{f}_c) \geq \frac{\alpha}{f_s \varsigma \pi^2} \quad (18c)$$

$$\text{var}(\hat{\phi}) \geq \frac{\alpha + 4\pi^2 f_c^2}{f_2 \alpha \varsigma} \quad (18d)$$

$$\text{var}(\hat{\beta}) \geq \frac{3\beta^2}{2f_s \varsigma} \quad (18e)$$

where  $\varsigma$  denotes the SNR, and  $f_s$  denotes the sampling frequency.

The CRLB provide intuitive insights on the estimation of parameters. The variance of any Gaussian echo parameter estimator depends on the SNR and sampling frequency. Higher SNR and sampling frequency will improve the accuracy of parameter estimation. Furthermore, the variances of estimators also depend on the spectral characteristics of the echo through the bandwidth factor and center frequency. For example, the variance of the TOF estimator (18b) inversely depends on the echo bandwidth. This implies that echoes with large bandwidth (or narrow timewidth) offer a more accurate TOF estimation. The variance of the center frequency estimator (18c) also depends on the bandwidth. The smaller the bandwidth (or the broader the timewidth), the more accurate is the center frequency estimation.

To assess the performance of estimation, we utilize a Monte-Carlo simulation to observe the means of estimators for bias and the variances of estimators against the CRLB. A Gaussian echo with bandwidth factor  $\alpha = 25$  (MHz)<sup>2</sup> (the 98% bandwidth is 1.91 MHz), arrival time  $\tau = 1$  μs, center frequency  $f_c = 5$  MHz, phase  $\phi = 1$  rad, and amplitude  $\beta = 1$ , summarized in a parameter vector,

$\theta = [25 \ 1 \ 5 \ 1 \ 1]$ , is simulated. A realization of a zero-mean WGN process with the variance  $\sigma^2$  is added to the echo. Then, the GN algorithm is applied to estimate echo parameters. This process is repeated 100 times, yielding a different estimate each time because of the random nature of the noise process. The means and variances of estimators are tabulated in Table II for echoes with SNR of 20, 10, 5, 2.5, and 1.25 dB. The actual echo parameters used in simulation and the initial guesses for parameters are also shown in the table. The Cramer-Rao analytical bounds, computed using (18a) to (18e) are located under the variance of the estimators for comparison. It can be observed that the means of the estimators nearly achieve the actual parameter vector, and the variances of the estimators attain the CRLB for SNR as low as 2.5 dB (see Table II). Hence, these estimators are the minimum-variance unbiased (MVU) estimators. In addition, this table indicates that when the SNR is 20 dB or better, the estimation of center frequency and arrival time is very accurate, i.e., the estimation errors are less than 0.01% of the actual values.

In summary, the maximum likelihood estimator  $\hat{\theta}$  is MVU and asymptotically distributed as normal distribution,  $\hat{\theta} \sim N(\theta, I^{-1}(\theta))$ , where  $I(\theta)$  is the Fisher information matrix evaluated at the true value of the parameter vector. That is, for large enough data records, on the average, the MLE achieves the true value of the parameters, and its covariance achieves the inverse Fisher information matrix [18]. This forms the basis for claiming the optimality of the estimated parameters.

Although the estimated parameters may be optimal, the degradation caused by noise is inevitable. The quantification of degradation is desirable for asserting the degree of confidence (resolution) on the estimated parameters. The knowledge of the bound on the variance of an estimator leads to a resolution bound, i.e., it can be determined from the standard deviation of the estimator (the square root of estimator variance, CRLB). That is, with a 90% confidence, the estimated parameter is expected to lie in the range  $\hat{\theta} \mp 2\Delta\hat{\theta}$ , where  $\Delta\hat{\theta}$  is the standard deviation. For example, consider the arrival time estimation of the echo with a SNR of 20 dB (Table II). The optimum estimator for arrival time has been found to be  $\hat{\tau} = 0.9999 \mu s$ , and its standard deviation is calculated as  $\Delta\hat{\tau} = 0.0014 \mu s$ . The confidence interval for the arrival time can be determined as the interval  $0.9998 \mp 0.0028 \mu s$ . We note that this is the best resolution that can be achieved in the presence of noise.

In conclusion, the MLE of the Gaussian echo parameters using GN and simplex search methods achieves the optimal solutions. The method also provides confidence intervals on the estimated parameters by evaluating their analytical CRLB at the values of estimated parameters.

## V. MLE OF M-SUPERIMPOSED ECHOES

It has been shown that the MLE of a Gaussian echo is optimal. However, the parameter estimation problem

becomes more complicated when the MLE of a number of superimposed Gaussian echoes is considered.

Consider the discrete version of the M-superimposed Gaussian echo model (3):

$$y = \sum_{m=1}^M s(\theta_m) + \nu \quad (19)$$

where  $s(\cdot)$  denotes the Gaussian echo model and  $\nu$  denotes a WGN sequence with variance  $\sigma_\nu^2$ . The parameter estimation problem is to estimate the parameter vectors  $\theta_1, \theta_2, \dots, \theta_M$  given the noisy observation of echoes, some of which may be overlapping. The direct LS approach to this problem requires minimization of the term:

$$\left\| y - \sum_{m=1}^M s(\theta_m) \right\|^2,$$

with respect to parameter vectors. This is a multidimensional optimization problem and requires search over  $M$  parameter vectors. The increased complexity may result in extra computational load and potential poor convergence.

As an alternative to LS methods, the EM algorithms have been proposed for parameter estimation of superimposed signals in noise [19]. The EM algorithms translate M-superimposed echoes estimation into M-separate echo estimations by using unobserved data sets. We define  $x_m$  as the “unobserved data” set for the  $m$ th echo under a WGN sequence  $\nu_m$  as

$$x_m = s(\theta_m) + \nu_m. \quad (20)$$

This unobserved data represent a single echo in WGN and relate to the observed data through a linear transformation

$$y = \sum_{m=1}^M x_m \quad (21)$$

where  $x_m$  and  $y$  are Gaussian random sequences. It has been proven that one can compute the MLE of the parameter vectors  $\theta_m$  subject to data sets  $x_m$  [19]. The MLE of  $\theta_m$  maximizes the pdf associated with the data set  $x_m$  (12). However, the data set  $x_m$  is not directly available. Given the linear transformation in (21), the expectation of  $x_m$  can be computed in terms of the observed data and the current value of the parameter vectors [19] as

$$\hat{x}_m^{(k)} = s(\theta_m^{(k)}) + \beta_m(y - \sum_{l=1}^M s(\theta_l^{(k)})), \text{ where } \sum_{m=1}^M \beta_m = 1. \quad (22)$$

This is basically the expectation step (E-Step) of the EM algorithm. The maximization step (M-Step) involves the maximization of the pdf associated with the corresponding parameter vector using the expected signal from the E-Step [20]. The M-Step iterates the parameter vector  $\theta_m^{(k)}$  by minimizing:

$$\theta_m^{(k+1)} = \arg_{\theta_m} \min \left\| \hat{x}_m^{(k)} - s(\theta_m) \right\|^2.$$

TABLE II  
COMPARISON OF THE CRLB AND THE VARIANCES OF ESTIMATORS FOR DIFFERENT SNR.  
MONTE CARLO SIMULATION RESULTS ARE OBTAINED USING 100 TRIALS.  
SAMPLING FREQUENCY IS 200 MHz.

	Bandwidth factor [(MHz) <sup>2</sup> ]	Arrival time (μs)	Center frequency (MHz)	Phase (rad)	Amplitude
Actual parameters	25.0000	1.0000	8.0000	1.0000	1.0000
Initial guess	20.0000	0.8000	6.4000	0.8000	0.8000
20.00-dB SNR					
Mean	25.0207	0.9999	7.9986	7.2797	1.0015
Variance	0.2435	1.62E-06	1.40E-04	0.0041	6.58E-05
CRLB	0.2443	1.95E-06	1.23E-04	0.0049	7.33E-05
10.00-dB SNR					
Mean	25.0325	0.9998	8.0027	7.2743	1.0038
Variance	2.5764	2.02E-05	0.0013	0.0527	7.00E-04
CRLB	2.4576	1.90E-05	0.0012	0.0501	7.00E-04
5.00-dB SNR					
Mean	25.7558	0.9996	8.0054	7.2701	1.0116
Variance	7.6806	6.18E-05	0.0043	0.1550	0.0026
CRLB	7.8200	6.25E-05	0.0039	0.1596	0.0023
2.50-dB SNR					
Mean	25.3903	0.9977	7.9957	7.1694	1.0095
Variance	13.7007	1.04E-04	0.0072	0.2663	0.0033
CRLB	14.0078	1.12E-04	0.0070	0.2859	0.0042
1.25-dB SNR					
Mean	25.5538	0.9985	7.9688	7.2529	1.0090
Variance	26.1400	9.45E-04	0.0610	1.0738	0.0138
CRLB	18.6700	3.10E-04	0.0095	0.3813	0.0056

In summary, the EM algorithm for parameter estimation of M-superimposed Gaussian echoes in WGN can be implemented in the following steps.

Step 1. Make initial guesses for the parameter vectors and form  $\Theta^{(0)} = [\theta_1^{(0)}; \theta_2^{(0)}; \dots; \theta_M^{(0)}]$ .

Set  $k = 0$  (iteration number).

Step 2. For  $m = 1, 2, \dots, M$  compute the expected echoes (E-Step):

$$\hat{x}_m^{(k)} = s(\theta_m^{(k)}) + \frac{1}{M} \left\{ y - \sum_{l=1}^M s(\theta_l^{(k)}) \right\}.$$

Step 3. For  $m = 1, 2, \dots, M$ , iterate the corresponding parameter vector (M-Step):

$$\theta_m^{(k+1)} = \arg_{\theta_m} \min \left\| \hat{x}_m^{(k)} - s(\theta_m) \right\|^2.$$

Step 4. Check convergence criterion:

if  $\left\| \Theta^{(k+1)} - \Theta^{(k)} \right\| \leq \text{tolerance}$ , then stop.

Step 5. Set  $k \rightarrow k + 1$  and go to Step 2.

In Step 2 (E-Step) of the algorithm, the expected signals are computed using the current estimate of the parameter vectors  $\theta_m^{(k)}$  and the observed data  $y$ . Then, using these expected signals, in the M-Step,  $\theta_m^{(k+1)}$ , is computed for each signal as the maximum likelihood estimate for  $\theta_m^{(k)}$ . In other words, the M-Step corresponds to the MLE of a single echo using the estimated data  $\hat{x}_m^{(k)}$ . Note that the

M-Step can be implemented using the GN algorithm developed earlier for single echo estimation. The initial guess for the algorithm would be the current estimate of the  $m$ th parameter set, and the data would be the expected signal for the  $m$ th echo. Then, the algorithm would return the MLE for the  $m$ th echo. Once the MLE for each echo is performed, in the next E-Step, the expectation of each echo  $\hat{x}_{m+1}^{(k)}$  will be computed using  $\theta_m^{(k+1)}$  and so on. The sequence of operations for iterations  $k = 1, 2, \dots, K$  can be diagrammed as

$$\Theta^{(0)} \xrightarrow{\text{Step } x_{1,2,\dots,M}^{(0)}} \Theta^{(1)} \xrightarrow{\text{Step } x_{1,2,\dots,M}^{(1)}} \dots \xrightarrow{\text{Step } x_{1,2,\dots,M}^{(K-1)}} \Theta^{(K)}.$$

After all of the parameters are updated, the norm of the improvement in parameter vectors is compared against a preset tolerance as the convergence criterion in Step 4 of the algorithm. If not convergence, Steps 2 and 3 will be repeated using estimated parameters from previous iteration.

#### A. SAGE Algorithm

It can be observed that the EM algorithm has a parallel computing structure that is at each step of the algorithm at which the expected signals are computed using the current estimate of parameter sets and the observed data. Then, the corresponding parameter sets are computed using those expected signals. One alternative to this parallel

structure is to update parameter sets right after the M-Step, without waiting for the other parameter vectors to be estimated. This incorporates the current estimate immediately into the E-Step and hopefully speeds up the convergence. This method is known as the generalized EM algorithm. It has been noted that, compared with regular EM, it has a faster convergence property [21]. For the case of WGN, this method is also known as space alternating generalized EM (SAGE) algorithm [22]. Similar to EM, the SAGE algorithm involves estimating an “expected signal” for each echo and then computing the MLE of the corresponding parameter set using the expected signal and the current value of parameters. This can be summarized in the following steps.

Step 1. Make initial guesses for the parameter vectors and form  $\Theta^{(0)} = [\theta_1^{(0)}; \theta_2^{(0)}; \dots; \theta_m^{(0)}]$ . Set  $k = 0$  (iteration number) and  $m = 1$  (echo number).

Step 2. Compute the expected signal for the  $m$ th echo (E-Step):

$$\hat{x}_m^{(k)} = s(\theta_m^{(k)}) + \frac{1}{M} \left\{ y - \sum_{l=1}^M s(\theta_l^{(k)}) \right\}.$$

Step 3. Iterate the  $m$ th parameter vector (M-Step):

$$\theta_m^{(k+1)} = \arg_{\theta_m} \min \left\| \hat{x}_m^{(k)} - s(\theta_m) \right\|^2 \text{ and}$$

set  $\theta_m^{(k)} = \theta_m^{(k+1)}$ .

Step 4. Set  $m \rightarrow m + 1$  and go to Step 2 unless  $m > M$ .

Step 5. Check convergence criterion:

if  $\|\Theta^{(k+1)} - \Theta^{(k)}\| \leq$  tolerance, then stop.

Step 6. Set  $m = 1$ ,  $k \rightarrow k + 1$ , and go to Step 2.

In Step 2 (E-Step), using the current estimate of the parameter vector  $\theta_m^{(k)}$  and the observed data  $y$ , the expectation of the  $m$ th echo,  $\hat{x}_m^{(k)}$ , is computed. Then, using this expected signal, in the M-Step,  $\theta_m^{(k+1)}$  is computed as the maximum likelihood estimate for  $\theta_m^{(k)}$ . In other words, the M-Step corresponds to the MLE of a single echo with the estimated data  $\hat{x}_m^{(k)}$ . Note that the M-Step can be carried out using the GN algorithm developed earlier for single echo estimation. Then, in the next E-Step, the expectation of the next signal  $\hat{x}_{m+1}^{(k)}$  will be computed using  $\theta_m^{(k+1)}$ . The sequence of operations for the first iteration can be diagrammed as

$$\begin{aligned} \theta_1^{(0)} &\xrightarrow{\text{Step}} x_1^{(0)} \\ M &\xrightarrow{\text{Step}} \theta_1^{(1)} \\ &\dots x_M^{(0)} \xrightarrow{\text{Step}} \theta_m^{(1)}. \end{aligned}$$

Once all of the parameters are updated, the convergence criterion as the norm of difference between two consecutive parameter sets is checked against the preset tolerance. If not convergence, Steps 2 through 4 will be repeated using estimated parameters from the previous iteration. The flow chart of the algorithm is given in Fig. 5.

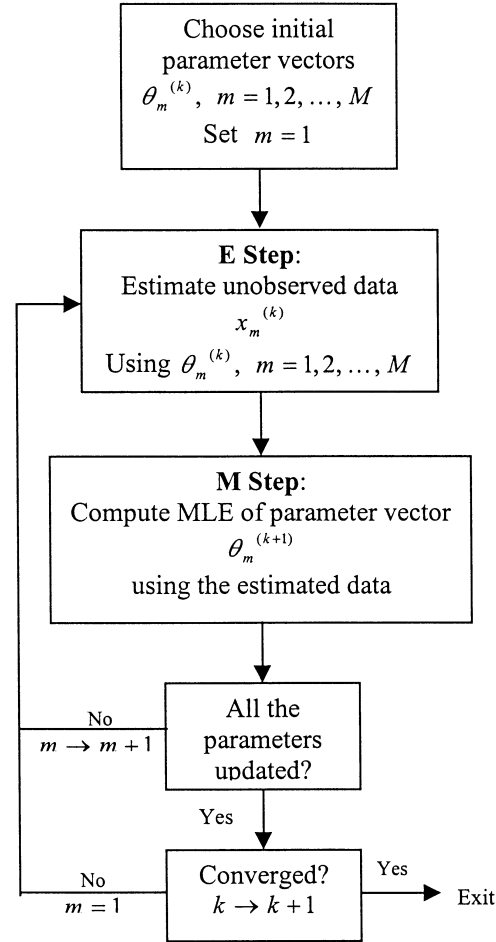


Fig. 5. The flow chart of the SAGE algorithm.

## B. Multiple Echo Estimation Results and Discussions

The SAGE algorithm has been tested on the simulated Gaussian echoes. We give an example of three non-interfering echoes (Fig. 6) and three interfering echoes (Fig. 7) in additive WGN. The parameter estimation results are tabulated in Table III for non-interfering echoes and in Table IV for interfering echoes. In the tables, the actual parameter vectors used in the simulation, the initial guesses for the parameter vectors, and the optimum parameter vectors computed by the algorithm are listed. For the case of three non-interfering echoes, the parameter estimation is robust, regardless of a poor initial guess (see Table III) and a significant noise level (the SNR is about 12 dB). The parameter estimation results support optimality, where the estimation SNR is about 31 dB.

For comparison of the SAGE algorithm with a LS algorithm, the estimation of the three non-interfering echoes (Fig. 6) is considered. The Levenberg-Marquardt [16] of LS, given the same initial guess as to SAGE (Table III), achieves the optimal solution. However, given an arbitrary initial guess, the convergence is not guaranteed. This is demonstrated using the example of three interfering echoes (Fig. 7). The initial guess listed in Table IV is supplied to both algorithms. The LS method fails to converge, but the

TABLE III  
 PARAMETER ESTIMATION RESULTS FOR THREE NON-INTERFERING ECHOES WITH A SNR OF 12.5 dB.  
 THE ESTIMATION SNR IS 31.60 dB. NUMBER OF ITERATIONS IS 33.

Echo parameters	Bandwidth factor [(MHz) <sup>2</sup> ]	Arrival time (μs)	Center frequency (MHz)	Phase (rad)	Amplitude
Actual parameters	15.0000	1.0000	8.0000	0.5200	1.0000
	12.0000	2.5000	7.5000	1.0400	0.9000
	10.0000	4.0000	7.0000	1.5700	0.8000
Initial guess	8.0000	0.8000	6.0000	0.0000	0.5000
	8.0000	2.3000	6.0000	0.0000	0.5000
	8.0000	3.7000	6.0000	0.0000	0.5000
Estimated parameters	15.5400	0.9964	7.9930	0.3220	1.0140
	12.1100	2.4970	7.4760	0.8976	0.9014
	9.7380	4.0000	7.0160	1.5910	0.7935

TABLE IV  
 PARAMETER ESTIMATION RESULTS FOR THREE INTERFERING ECHOES WITH A SNR OF 10.7 dB.  
 THE ESTIMATION SNR IS 14.69 dB. NUMBER OF ITERATIONS IS 335.

Echo parameters	Bandwidth factor [(MHz) <sup>2</sup> ]	Arrival time (μs)	Center frequency (MHz)	Phase (rad)	Amplitude
Actual parameters	10.0000	1.5000	5.0000	1.0000	0.9000
	9.0000	2.0000	7.0000	0.0000	1.0000
	8.0000	2.5000	6.0000	0.0000	0.8000
Initial guess	8.0000	1.5000	6.0000	0.0000	0.5000
	8.0000	1.5000	6.0000	0.0000	0.5000
	8.0000	1.5000	6.0000	0.0000	0.5000
Estimated parameters	10.8900	1.5130	4.9990	1.3760	0.9290
	8.8370	1.9980	7.0420	0.1232	0.9818
	7.4050	2.4970	5.9690	0.1209	0.8099

TABLE V  
 PARAMETER ESTIMATION RESULTS FOR TWO CLOSELY SPACED OVERLAPPING ECHOES WITH A SNR OF 11.7 dB.  
 THE ESTIMATION SNR IS 28 dB. NUMBER OF ITERATIONS IS 889.

Echo parameters	Bandwidth factor [(MHz) <sup>2</sup> ]	Arrival time (μs)	Center frequency (MHz)	Phase (rad)	Amplitude
Actual parameters	20.0000	0.9000	5.6000	0.0000	1.0000
	16.0000	1.1000	4.3000	1.9000	0.8000
Initial guess	25.0000	1.0000	6.0000	0.0000	1.2000
	25.0000	1.0000	6.0000	0.0000	1.2000
Estimated parameters	19.8200	0.9094	5.6300	0.3200	0.9812
	16.6200	1.1030	4.3200	2.0040	0.7807

TABLE VI  
 PARAMETER ESTIMATION RESULTS FOR EXPERIMENTAL NON-INTERFERING ECHOES.  
 THE SNR AFTER ESTIMATION IS 21.26 dB. NUMBER OF ITERATIONS IS 64.

Echo parameters	Bandwidth factor [(MHz) <sup>2</sup> ]	Arrival time (μs)	Center frequency (MHz)	Phase (rad)	Amplitude
Initial guess	10.000	2.000	5.000	0.000	0.800
	10.000	5.000	5.000	0.000	0.800
Estimated parameters	25.940	1.755	5.583	1.068	1.044
	26.730	5.049	5.484	0.783	0.517

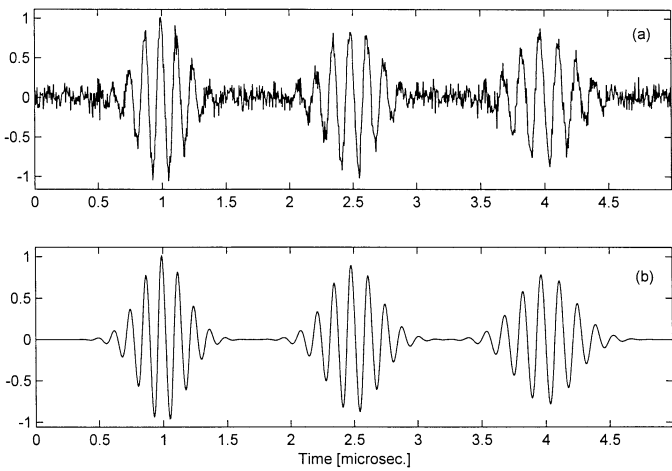


Fig. 6. a) Three non-interfering echoes with a SNR of 12.5 dB; b) estimated echoes for (a).

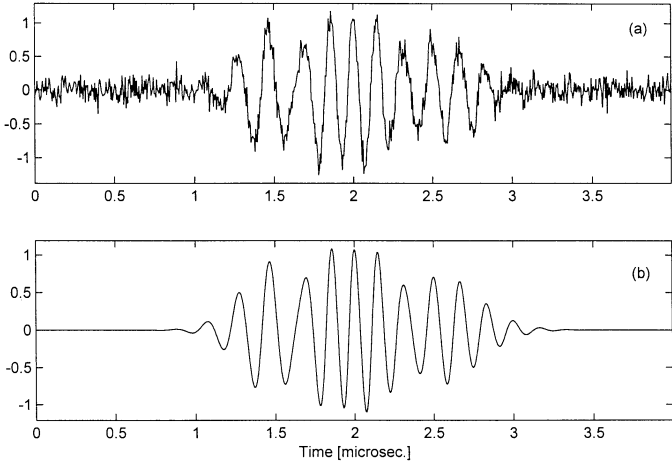


Fig. 7. a) Three interfering echoes with a SNR of 10.7 dB; b) estimated echoes for (a).

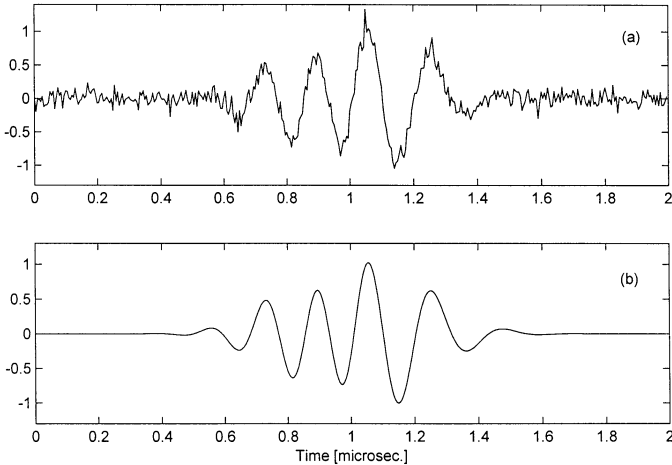


Fig. 8. a) Two closely spaced overlapping echoes with a SNR of 11.7 dB; b) estimated echoes for (a).

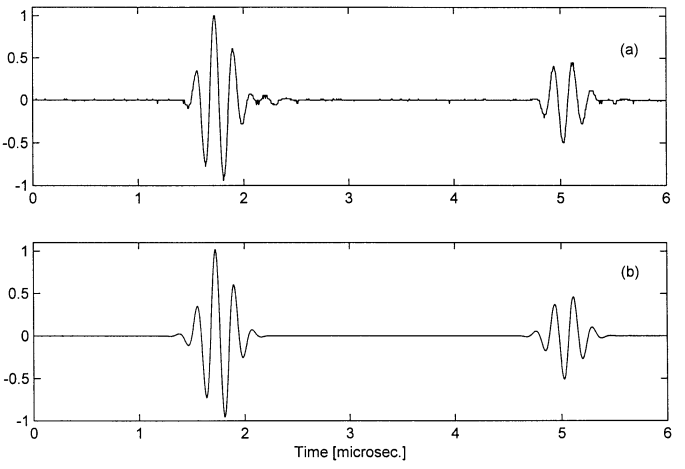


Fig. 9. a) Two non-interfering echoes reflected from the plexiglass sample (4.8-mm thick); b) estimated echoes for (a).

SAGE algorithm achieves convergence. Note that the same initial guess is used for the parameters of all three echoes (see Table IV). It is known that the LS methods are sensitive to the initial guess, i.e., only those initial guesses that are close to optimum result in convergence. It is observed that the SAGE method is far less sensitive to initial starting point compared with the LS methods (see Table IV). This argument can be attributed to the fact that the LS method tries to fit M echoes simultaneously to the observed data; the SAGE method tries to fit one echo at a time to the unobserved data sets. However, the estimation of the unobserved data brings about extra computation and makes convergence slow. It can be verified that the LS method converges faster than the SAGE method does if the initial guess is near optimum.

Another shortcoming of the LS method is that it is inefficient to discriminate closely spaced overlapping echoes. The SAGE algorithm does better than the LS method because it is able to differentiate the data sets associated with the individual echoes (unobserved data). Consider a simulation example (Fig. 8) consisting of two closely spaced overlapping echoes in time. The LS method fails to resolve the composing echoes given any initial guess; but the SAGE algorithm succeeds given a fair initial guess (Table V). However, the differentiation of the data points for unobserved data sets is difficult because of the overlap. Nevertheless, the SAGE algorithm is able to resolve the overlapping echoes at the cost of significant iteration. The optimal convergence (a desirable outcome) in this case is traded over the computational complexity.

In this study, the SAGE algorithm has also been tested on the experimental data. Fig. 9(a) shows the measured echoes reflected from the front and back surfaces of a plexiglass plate (4.8 mm thick). Fig. 9(b) shows the estimated echoes by the SAGE algorithm. Parameter estimation results are listed in Table VI in terms of the initial guess used in the algorithm, the estimation SNR, and the number of iterations. The estimated echoes are in good agreement with the experimental echoes when the estima-

tion SNR is about 21 dB. The parameters of estimated echoes offer conceptual interpretations for physical characteristics of the sample. The TDOA of the echoes can be linked to the thickness, and the amplitudes of echoes can be linked to the reflection and transmission coefficients. On the other hand, the center frequency and bandwidth factor of the second echo with reference to the first echo can be linked to the frequency-dependent attenuation. A more detailed investigation for parameter estimation of experimental echoes is presented in the application part of this study (see Part II).

## VI. CONCLUSIONS

In this study, we developed a model-based estimation method for analysis and system identification of ultrasonic backscattered echoes. The method is based on the Gaussian echo model whose parameters represent certain signal characteristics (TOF, bandwidth, frequency, phase, and amplitude) of an ultrasonic echo. Consequently, the backscattered echoes can be represented by the sum of Gaussian echoes had their parameters been accurately estimated. Then, we addressed the MLE of the Gaussian echo parameters in the presence of noise. First, we developed a fast GN algorithm for parameter estimation of a Gaussian echo in WGN. Through Monte-Carlo simulation, we have shown that the estimated parameters are unbiased, and their variances achieve the analytical CRLB. Consequently, the estimated parameters are said to be optimal. Then, the problem is generalized to the estimation of M-superimposed Gaussian echoes in WGN. However, this problem cannot be solved efficiently using a simple LS optimization method because of the increased complexity of the problem. Alternative to LS methods, the SAGE algorithm is proposed. The SAGE algorithm translates the M-echo estimation problem into one-echo estimation problems, providing computational versatility. The algorithm has been shown to be superior to the LS optimization methods in that it is less dependent on the initial guess and able to resolve closely spaced overlapping echoes. The algorithm has also been tested on the experimental ultrasonic echoes reflected from planar surfaces. We have observed that the model-based estimation method achieves a very good representation of the measured echoes. This representation leads to a quantitative evaluation of ultrasonic echoes in terms of temporal and spectral characteristics. Furthermore, the estimated parameters have intuitive meanings for reflection and frequency-dependent attenuation and, hence, can be used for system identification. The potential NDE applications of the model-based estimation method are presented in Part II of this paper.

## APPENDIX A ANALYTICAL DERIVATION OF GRADIENTS, FISHER INFORMATION MATRIX, AND CRLB BOUNDS

The Gaussian echo model is defined by

$$s(t; \theta) = \beta e^{-\alpha(t-\tau)^2} \cos\{2\pi f_c(t-\tau) + \phi\} \quad 0 \leq t \leq T_s \quad (\text{A1})$$

where  $\theta = [\alpha \ \tau \ f_c \ \phi \ \beta]$  denotes the parameter vector. The echo is assumed to exist in the interval  $[0, T_s]$  and has a bandpass characteristic. To simplify analytical derivations, we consider the following kernel functions:

$$\begin{aligned} f(t; \theta) &= e^{-\alpha(t-\tau)^2} \cos\{2\pi f_c(t-\tau) + \phi\} \\ g(t; \theta) &= e^{-\alpha(t-\tau)^2} \sin\{2\pi f_c(t-\tau) + \phi\}. \end{aligned}$$

The partial derivatives of the Gaussian echo in terms of the kernel functions can be written as

$$\frac{\partial s(t; \theta)}{\partial \alpha} = -\beta(t-\tau)^2 f(t; \theta) \quad (\text{A2})$$

$$\frac{\partial s(t; \theta)}{\partial \tau} = 2\alpha\beta(t-\tau)f(t; \theta) + 2\pi f_c \beta g(t; \theta) \quad (\text{A3})$$

$$\frac{\partial s(t; \theta)}{\partial f_c} = -2\pi\beta(t-\tau)g(t; \theta) \quad (\text{A4})$$

$$\frac{\partial s(t; \theta)}{\partial \phi} = -\beta g(t; \theta) \quad (\text{A5})$$

$$\frac{\partial s(t; \theta)}{\partial \beta} = f(t; \theta). \quad (\text{A6})$$

The Fisher information matrix is defined as (17):

$$I(\theta) = \frac{1}{\sigma^2} H^T(\theta) H(\theta) \quad (\text{A7})$$

where  $H(\theta)$  denotes the gradient matrix. The gradient matrix can be written in terms of partial derivatives:

$$H(\theta) = \left[ \begin{array}{ccccc} \frac{\partial \bar{s}}{\partial \alpha} & \frac{\partial \bar{s}}{\partial \tau} & \frac{\partial \bar{s}}{\partial f_c} & \frac{\partial \bar{s}}{\partial \phi} & \frac{\partial \bar{s}}{\partial \beta} \end{array} \right]$$

where  $\bar{s}$  denotes the discrete signal vector obtained by sampling the continuous signal (A1) with a sampling frequency of  $f_g$ . The elements of the matrix  $H^T(\theta) H(\theta)$  can be written as an inner product of partial derivatives:

$$[H^T(\theta) H(\theta)]_{ij} = \left[ \frac{\partial \bar{s}}{\partial \theta_i} \right]^T \left[ \frac{\partial \bar{s}}{\partial \theta_j} \right]$$

where  $\theta_i$  denotes the  $i$ th parameter in the parameter vector. The inner products of partial derivatives can be calculated by using their corresponding analytical derivatives given in (A2)–(A6). Each element can be computed explicitly using the following approximation:

$$\left[ \frac{\partial \bar{s}}{\partial \theta_i} \right]^T \left[ \frac{\partial \bar{s}}{\partial \theta_j} \right] \cong f_s \int_{-\infty}^{\infty} \frac{\partial s(t; \theta)}{\partial \theta_i} \frac{\partial s(t; \theta)}{\partial \theta_j} dt.$$

This expression is written based on the fact that the sum of the discrete samples of a continuous signal in its interval is equivalent to sampling frequency times its analytical integration. To simplify mathematical expressions, we define the following variables:

$$A_{ij} = \int_{-\infty}^{\infty} \frac{\partial s(t; \theta)}{\partial \theta_i} \frac{\partial s(t; \theta)}{\partial \theta_j} dt.$$

We note that  $A_{ij} = A_{ji}$ . Hence, the following integrals need to be calculated to compute the Fisher information matrix:

$$\begin{aligned} A_{11} &= \beta^2 \int_{-\infty}^{\infty} (t - \tau)^4 f^2(t; \theta) dt \\ A_{12} &= -2\alpha\beta^2 \int_{-\infty}^{\infty} (t - \tau)^3 f^2(t; \theta) dt \\ &\quad - 2\pi f_c \beta^2 \int_{-\infty}^{\infty} (t - \tau)^2 f(t; \theta) g(t; \theta) dt \\ A_{13} &= 2\pi\beta^2 \int_{-\infty}^{\infty} (t - \tau)^3 f(t; \theta) g(t; \theta) dt \\ A_{14} &= \beta^2 \int_{-\infty}^{\infty} (t - \tau)^2 f(t; \theta) g(t; \theta) dt \\ A_{15} &= -\beta \int_{-\infty}^{\infty} (t - \tau)^2 f^2(t; \theta) dt \\ A_{22} &= (2\alpha\beta)^2 \int_{-\infty}^{\infty} (t - \tau)^2 f^2(t; \theta) dt + (2\pi f_c \beta)^2 \\ &\quad \cdot \int_{-\infty}^{\infty} g^2(t; \theta) dt + 8\pi\alpha f_c \beta^2 \int_{-\infty}^{\infty} (t - \tau) f(t; \theta) g(t; \theta) dt \\ A_{23} &= -4\alpha\pi\beta^2 \int_{-\infty}^{\infty} (t - \tau)^2 f(t; \theta) g(t; \theta) dt \\ &\quad - (2\pi\beta)^2 f_c \int_{-\infty}^{\infty} g^2(t; \theta) dt \\ A_{24} &= -2\alpha\beta^2 \int_{-\infty}^{\infty} (t - \tau) f(t; \theta) g(t; \theta) dt \\ &\quad - 2\pi f_c \beta^2 \int_{-\infty}^{\infty} g^2(t; \theta) dt \end{aligned}$$

$$\begin{aligned} A_{25} &= 2\alpha\beta \int_{-\infty}^{\infty} (t - \tau) f^2(t; \theta) dt \\ &\quad + 2\pi f_c \beta \int_{-\infty}^{\infty} f(t; \theta) g(t; \theta) dt \\ A_{33} &= (2\pi\beta)^2 \int_{-\infty}^{\infty} (t - \tau)^2 g^2(t; \theta) dt \\ A_{34} &= 2\pi\beta^2 \int_{-\infty}^{\infty} (t - \tau) g^2(t; \theta) dt \\ A_{35} &= -2\pi\beta \int_{-\infty}^{\infty} (t - \tau) f(t; \theta) g(t; \theta) dt \\ A_{44} &= \beta^2 \int_{-\infty}^{\infty} g^2(t; \theta) dt \\ A_{45} &= -\beta \int_{-\infty}^{\infty} f(t; \theta) g(t; \theta) dt \\ A_{55} &= \int_{-\infty}^{\infty} f^2(t; \theta) dt. \end{aligned}$$

These integrals can be simplified using Gaussian echo properties. It can be shown that the orthogonality principle holds for the kernel functions:

$$\int_{-\infty}^{\infty} f(t; \theta) g(t; \theta) dt = 0.$$

This makes  $A_{13}, A_{14}, A_{35}, A_{45} = 0$ . We define the normalized signal energy (6) as

$$\overline{E}_s = \int_{-\infty}^{\infty} f^2(t; \theta) dt = \int_{-\infty}^{\infty} g^2(t; \theta) dt = \frac{1}{2} \sqrt{\frac{\pi}{2\alpha}} \left( 1 + e^{-\frac{-f_c^2}{(\alpha/2\pi^2)}} \right).$$

For the bandpass condition, this energy equation simplifies to

$$\overline{E}_s = \frac{1}{2} \sqrt{\frac{\pi}{2\alpha}}.$$

Then, the energy of the model echo, in terms of the normalized energy, can be written as

$$E_s = \beta^2 \overline{E}_s.$$

Using this property, the following elements can be calculated:

$$A_{44} = \beta^2 \overline{E}_s \text{ and } A_{55} = \overline{E}_s.$$

Using even and odd function integration properties, it can be shown that

$$\int_{-\infty}^{\infty} (t - \tau)^3 f^2(t; \theta) dt = 0 \text{ and } \int_{-\infty}^{\infty} (t - \tau) g^2(t; \theta) dt = 0.$$

These properties make  $A_{12}, A_{23}, A_{25}, A_{34} = 0$ . The following integrals can be calculated in the Fourier domain:

$$\int_{-\infty}^{\infty} (t - \tau)^2 f^2(t; \theta) dt = \frac{\bar{E}_s}{4\alpha} \text{ and } \int_{-\infty}^{\infty} (t - \tau)^4 f^2(t; \theta) dt = \frac{3\bar{E}_s}{16\alpha^2}.$$

Utilizing these properties, we can obtain explicit solutions for the following elements:

$$\begin{aligned} A_{11} &= \beta^2 \frac{3\bar{E}_s}{16\alpha^2} \\ A_{15} &= -\beta \frac{\bar{E}_s}{4\alpha} \\ A_{22} &= (2\alpha\beta)^2 \frac{\bar{E}_s}{4\alpha} + (2\pi f_c \beta)^2 \bar{E}_s \\ A_{24} &= -2\pi f_c \beta^2 \bar{E}_s \\ A_{33} &= (2\pi\beta)^2 \frac{\bar{E}_s}{4\alpha}. \end{aligned}$$

Using all of the calculated elements,  $H^T(\theta)H(\theta)$  becomes

$$H^T(\theta)H(\theta) = f_s E_s \begin{bmatrix} \frac{3}{16\alpha^2} & 0 & 0 & 0 & \frac{-1}{4\alpha\beta} \\ 0 & \alpha + (2\pi f_c)^2 & 0 & -2\pi f_c & 0 \\ 0 & 0 & \frac{\pi^2}{\alpha} & 0 & 0 \\ 0 & -2\pi f_c & 0 & 1 & 0 \\ \frac{-1}{4\alpha\beta} & 0 & 0 & 0 & \frac{1}{\beta^2} \end{bmatrix}.$$

Finally, the inverse of this expression can also be carried out analytically as:

$$[H^T(\theta)H(\theta)]^{-1} = \frac{1}{f_s E_s} \begin{bmatrix} 8\alpha^2 & 0 & 0 & 2\alpha\beta & \\ 0 & \frac{1}{\alpha} & 0 & \frac{2\pi f_c}{\alpha} & 0 \\ 0 & 0 & \frac{\pi^2}{\alpha} & 0 & 0 \\ 0 & \frac{2\pi f_c}{\alpha} & 0 & \frac{\alpha + (2\pi f_c)^2}{\alpha} & 0 \\ 2\alpha\beta & 0 & 0 & 0 & \frac{3\beta^2}{2} \end{bmatrix}. \quad (\text{A8})$$

Then, the Fisher information matrix (A7) can be written as

$$I(\theta) = \left( \frac{f_s E_s}{\sigma^2} \right) \begin{bmatrix} \frac{3}{16\alpha^2} & 0 & 0 & 0 & \frac{-1}{4\alpha\beta} \\ 0 & \alpha + (2\pi f_c)^2 & 0 & -2\pi f_c & 0 \\ 0 & 0 & \frac{\pi^2}{\alpha} & 0 & 0 \\ 0 & -2\pi f_c & 0 & 1 & 0 \\ \frac{-1}{4\alpha\beta} & 0 & 0 & 0 & \frac{1}{\beta^2} \end{bmatrix} \quad (\text{A9})$$

where  $E_s$  denotes the signal energy,  $\sigma^2$  denotes the noise variance, and  $f_s$  denotes the sampling frequency. The ratio,  $\varsigma = \frac{E_s}{\sigma^2}$ , in (A9) is recognized as the SNR, where  $\sigma^2$  is defined as the noise energy for WGN. This matrix can be inverted analytically to obtain the inverse Fisher information matrix:

$$I^{-1}(\theta) = \frac{1}{f_s \varsigma} \begin{bmatrix} 8\alpha^2 & 0 & 0 & 0 & 2\alpha\beta \\ 0 & \frac{1}{\alpha} & 0 & \frac{2\pi f_c}{\alpha} & 0 \\ 0 & 0 & \frac{\pi^2}{\alpha} & 0 & 0 \\ 0 & \frac{2\pi f_c}{\alpha} & 0 & \frac{\alpha + (2\pi f_c)^2}{\alpha} & 0 \\ 2\alpha\beta & 0 & 0 & 0 & 1.5\beta^2 \end{bmatrix}. \quad (\text{A10})$$

Hence, in terms of SNR,  $\varsigma$ , the terms along the diagonal of the inverse Fisher information matrix yield the analytical CRLB on the variances of parameters:

$$\text{var}(\hat{\alpha}) \geq \frac{8\alpha^2}{f_s \varsigma} \quad (\text{A11})$$

$$\text{var}(\hat{\tau}) \geq \frac{1}{f_s \varsigma \alpha} \quad (\text{A12})$$

$$\text{var}(\hat{f}_c) \geq \frac{\alpha}{f_s \varsigma \pi^2} \quad (\text{A13})$$

$$\text{var}(\hat{\phi}) \geq \frac{\alpha + (2\pi f_c)^2}{f_s \varsigma \alpha} \quad (\text{A14})$$

$$\text{var}(\hat{\beta}) \geq \frac{3\beta^2}{2f_s \varsigma}. \quad (\text{A15})$$

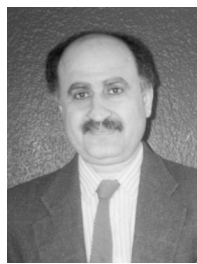
## REFERENCES

- [1] J. A. Jensen, "A model for the propagation and scattering of ultrasound in tissue," *J. Acoust. Soc. Amer.*, vol. 89, no. 1, pp. 182–190, Jan. 1991.
- [2] J. Saniie, "Ultrasonic signal processing: System identification and parameter estimation of reverberant and inhomogeneous targets," Ph.D. dissertation, Purdue University, Aug. 1981.
- [3] A. Hein and W. D. O'Brien, "Current time-domain methods for assessing tissue motion by analysis from reflected ultrasound echoes," *IEEE Trans. Ultrason., Ferroelect., Freq. Contr.*, vol. 40, no. 2, pp. 84–102, Mar. 1993.
- [4] E. J. Chen, W. K. Jenkins, and W. D. O'Brien, "The impact of various imaging parameters on ultrasonic displacement and velocity estimates," *IEEE Trans. Ultrason., Ferroelect., Freq. Contr.*, vol. 41, no. 3, pp. 293–301, May 1994.

- [5] M. Sandell and A. Grennberg, "Estimation of the spatial impulse response of an ultrasonic transducer using a tomographic approach," *J. Acoust. Soc. Amer.*, vol. 98, no. 4, pp. 2094–2103, Oct. 1995.
- [6] H. Ericson, P. O. Borjesson, P. Odling, and N. G. Holmer, "A robust correlation receiver for distance estimation," *IEEE Trans. Ultrason., Ferroelect., Freq. Contr.*, vol. 40, no. 5, pp. 596–603, Sep. 1994.
- [7] A. K. Nandi, "On the subsample time delay estimation of narrowband ultrasonic echoes," *IEEE Trans. Ultrason., Ferroelect., Freq. Contr.*, vol. 42, no. 6, pp. 993–1001, Nov. 1995.
- [8] C. Martin, J. J. Meister, M. Ardit, and P. A. Farine, "A novel homomorphic processing of ultrasonic echoes for layer thickness measurement," *IEEE Trans. Signal Processing*, vol. 40, no. 7, pp. 1819–1825, Jul. 1992.
- [9] A. Grennberg and M. Sandell, "Estimation of subsample time delay differences in narrowband ultrasonic echoes using the hilbert transform correlation," *IEEE Trans. Ultrason., Ferroelect., Freq. Contr.*, vol. 41, no. 5, pp. 588–595, Sep. 1994.
- [10] K. W. Ferrera, R. Algazi, and J. Liu, "The effect of frequency dependent scattering and attenuation on the estimation of blood velocity using ultrasound," *IEEE Trans. Ultrason., Ferroelect., Freq. Contr.*, vol. 39, no. 6, pp. 754–767, Nov. 1992.
- [11] J. Saniie and D. T. Nagle, "Analysis of order-statistic CFAR threshold estimator for improved ultrasonic flaw detection," *IEEE Trans. Ultrason., Ferroelect., Freq. Contr.*, vol. 39, no. 5, pp. 618–630, Sep. 1992.
- [12] J. M. Girault, F. Ossant, A. Ouahabi, D. Kouame, and F. Patat, "Time-varying autoregressive spectral estimation for ultrasonic attenuation in tissue characterization," *IEEE Trans. Ultrason., Ferroelect., Freq. Contr.*, vol. 45, no. 3, pp. 650–659, May 1998.
- [13] D. L. Liu and M. Saito, "A new method for estimating the acoustic attenuation coefficient of tissue from reflected ultrasound signals," *IEEE Trans. Med. Imag.*, vol. 8, no. 1, pp. 107–110, Mar. 1989.
- [14] K. A. Wear, R. F. Wagner, and B. S. Garra, "A comparison of autoregressive spectral estimation algorithms and order determination methods in ultrasonic tissue characterization," *IEEE Trans. Ultrason., Ferroelect., Freq. Contr.*, vol. 42, no. 4, pp. 709–716, Jul. 1995.
- [15] J. A. Nelder and R. Mead, "A simplex method for function minimization," *Computer J.*, vol. 7, pp. 308–313, 1967.
- [16] K. P. Chong and S. H. Zak, *An Introduction to Optimization*. New York: John Wiley & Sons, Inc., 1996.
- [17] R. Demirli and J. Saniie, "Modeling and parameter estimation of ultrasonic backscattered echoes," in *Rev. Progress Quantitative Nondestructive Eval. Conf. Proc.*, vol. 15, 1995.
- [18] S. M. Kay, *Fundamentals of Statistical Signal Processing*. Prentice Hall, 1993.
- [19] M. Feder and E. Weinstein, "Parameter estimation of superimposed signals using the EM algorithm," *IEEE Trans. Acoust. Speech Signal Processing*, vol. 36, no. 4, pp. 477–489, Apr. 1988.
- [20] T. K. Moon, "The expectation-maximization algorithm," *IEEE Signal Processing Mag.*, pp. 47–60, Nov. 1996.
- [21] J. A. Fessler and A. O. Hero, "Complete-data spaces and generalized EM algorithms," in *Proc. IEEE Conf. Acoust., Speech, Signal Processing*, vol. 4, 1993, pp. 1–4.
- [22] I. Ziskind and M. Wax, "Maximum likelihood localization of multiple sources by alternating projection," *IEEE Trans. Acoust. Speech Signal Processing*, vol. 36, no. 10, pp. 1553–1560, Oct. 1988.



**Ramazan Demirli** (S'01) was born in Isparta, Turkey on November 11, 1970. He received the B.Sc. degree in electronics and communications engineering from the University of Uludag, Bursa, Turkey in 1991. In 1993, Mr. Demirli was awarded a scholarship by the Turkish Ministry of Education to pursue his graduate studies abroad. He received his M.S. degree in electrical and computer engineering from the Illinois Institute of Technology, Chicago, Illinois in 1995. Since then, he has been studying for his Ph.D. degree in the area of signal processing and ultrasonic imaging. In 2000, Mr. Demirli joined BrainMedia LLC, NY, as a principal systems engineer, where he conducts research in signal processing and data compression. His research interests include statistical signal processing, image processing, and superimposed signal estimation. Ramasam Demirli is a student member of IEEE.



**Jafar Saniie** (S'80–M'81–M'83–SM'91) was born in Iran on March 21, 1952. He received his B.S. degree in electrical engineering from the University of Maryland in 1974. He received his M.S. degree in biomedical engineering in 1977 from Case Western Reserve University, and he received his Ph.D. degree in electrical engineering from Purdue University.

In 1981, Dr. Saniie joined the Department of Applied Physics, University of Helsinki, Finland, to conduct research in photothermal and photoacoustic imaging. Since 1983, he has been with the Department of Electrical and Computer Engineering at Illinois Institute of Technology, where he is Professor and Director of the Ultrasonic Information Processing Laboratory. Dr. Saniie's research interests and activities are in ultrasonic signal and image processing, statistical pattern recognition, estimation and detection, and ultrasonic nondestructive testing. In particular, he has performed extensive work in the areas of frequency diverse ultrasonic flaw enhancement techniques, nonlinear signal processing in target detection, ultrasonic imaging of reverberant multilayer structures, morphological processing and pattern recognition in ultrasonic imaging, time-frequency analysis of ultrasonic signals, and application of neural networks for detecting flaw echoes and classifying microstructural scattering. Dr. Saniie has been a Technical Committee Member of the IEEE Ultrasonics Symposium since 1987, Program Coordinator of the Conference on Properties and Applications of Magnetic Materials since 1985, Editorial Advisory Member of the *Nondestructive Testing and Evaluation Journal* (1986–1996), and Associate Editor of the *IEEE Transactions on Ultrasonics, Ferroelectrics, and Frequency Control* since 1994. He is a member of Sigma Xi, IEEE, Tau Beta Pi, and Eta Kappa Nu and has been the IEEE Branch Counselor (1983–1990). He is the 1986 recipient of the Outstanding IEEE Student Counselor Award.